

See discussions, stats, and author profiles for this publication at: <https://www.researchgate.net/publication/258034220>

# 2'-Deoxyuridine 5'-Monophosphate Substrate Displacement in Thymidylate Synthase through 6-Hydroxy-2H-naphtho[1,8-bc]furan-2-one Derivatives

ARTICLE in JOURNAL OF MEDICINAL CHEMISTRY · OCTOBER 2013

Impact Factor: 5.45 · DOI: 10.1021/jm4014086 · Source: PubMed

READS

34

10 AUTHORS, INCLUDING:



Rosaria Luciani

Università degli Studi di Modena e Reggio Emilia

15 PUBLICATIONS 130 CITATIONS

SEE PROFILE



Cecilia Pozzi

Università degli Studi di Siena

14 PUBLICATIONS 88 CITATIONS

SEE PROFILE



Stefano Mangani

Università degli Studi di Siena

144 PUBLICATIONS 3,291 CITATIONS

SEE PROFILE



Maria Paola Costi

Università degli Studi di Modena e Reggio Emilia

112 PUBLICATIONS 1,100 CITATIONS

SEE PROFILE

# 2'-Deoxyuridine 5'-Monophosphate Substrate Displacement in Thymidylate Synthase through 6-Hydroxy-2*H*-naphtho[1,8-*bc*]furan-2-one Derivatives

Stefania Ferrari,<sup>†</sup> Samuele Calò,<sup>†</sup> Rosalida Leone,<sup>‡,§</sup> Rosaria Luciani,<sup>†</sup> Luca Costantino,<sup>†</sup> Susan Sammak,<sup>†</sup> Flavio Di Pisa,<sup>‡</sup> Cecilia Pozzi,<sup>‡</sup> Stefano Mangani,<sup>‡</sup> and M. Paola Costi<sup>\*,†</sup>

<sup>†</sup>Department of Life Sciences, University of Modena and Reggio Emilia, Via Campi 183, 41125 Modena, Italy

<sup>‡</sup>Department of Chemistry, University of Siena, Via Aldo Moro 2, 53100 Siena, Italy

## **S** Supporting Information

**ABSTRACT:** Thymidylate synthase (TS) is a target for antifolate-based chemotherapies of microbial and human diseases. Here, ligand-based, synthetic, and X-ray crystallography studies led to the discovery of 6-(3-cyanobenzoyloxy)-2-oxo-2*H*-naphtho[1,8-*bc*]furan, a novel inhibitor with a  $K_i$  of 310 nM against *Pneumocystis carinii* TS. The X-ray ternary complex with *Escherichia coli* TS revealed, for the first time, displacement of the substrate toward the dimeric protein interface, thus providing new opportunities for further design of specific inhibitors of microbial pathogens.

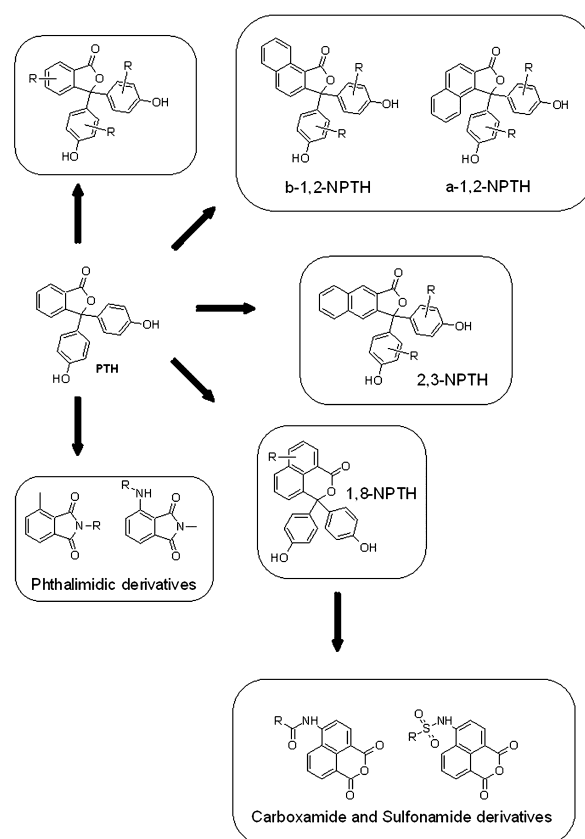
## ■ INTRODUCTION

Thymidylate synthase (TS) (EC: 2.1.1.45) catalyzes the reductive methylation of 2'-deoxyuridine 5'-monophosphate (dUMP) to 2'-deoxythymidine 5'-monophosphate (dTMP), assisted by the cofactor *N*5,*N*10-methylene tetrahydrofolate (MTHF).<sup>1</sup> Because TS represents the only synthetic source of dTMP in human cells, it is a potential target for designing chemotherapeutic agents. Classical TS inhibitors are used as anticancer agents and belong to the classical antimetabolite class. Examples of these drugs include 5-fluorouracil, which is a prodrug and is metabolized to the corresponding 5-fluorodeoxyuridine 5'-monophosphate (FdUMP) and raltitrexed (ZD1694).<sup>1–3</sup>

Phenolnaphthalen scaffolds have been used to explore the inhibition of TS through non-folate analogues. Stemming from phenolphthalein (PTH), which inhibits *Lactobacillus casei* TS (LcTS) with a  $K_i$  of 7  $\mu$ M,<sup>4</sup> a series of derivatives were designed and studied through the following different approaches: (I) chemical modification of phenols;<sup>5</sup> (II) growing of the core moiety to the 1,2-,<sup>6,7</sup> 1,8-,<sup>6,8–12</sup> and 2,3-<sup>9</sup>naphthalen compounds (1,2-NPTH, 1,8-NPTH, and 2,3-NPTH, respectively); (III) fragmentation and hopping to phthalimidic, carboxamide and sulfonamide derivatives of 1,8-naphthalic anhydride<sup>13,14</sup> (Scheme 1).

A number of interesting compounds emerged from these studies. MR36 (6-bromo-3,3-bis(3-chloro-4-hydroxyphenyl)-1*H*,3*H*-naphtho[1,8-*cd*]pyran-1-one) is under investigation as an anticancer compound against melanoma cell lines.<sup>11,12</sup> Sulfonamide derivatives of 1,8-naphthalic anhydride have shown low nanomolar  $K_i$  against human TS (hTS) and are being studied for cancer cell inhibition.<sup>14</sup> Compounds a156 (3,3-bis(3-chloro-4-hydroxyphenyl)-3*H*-benzo[*de*]isochromen-1-one) and GA9 (3,3-bis(3-bromo-4-hydroxyphenyl)-7-chloro-3*H*-benzo[*de*]isochromen-1-one) have shown species-specific inhibition profiles. Compound a156 has demonstrated antibacterial activity against vancomycin-resistant infections

Scheme 1. PTH-Derived Compounds



caused by Gram-positive bacteria, such as *Staphylococcus aureus*, and possesses low toxicity to human cells.<sup>6–10</sup> Previously

Received: September 12, 2013

Published: October 22, 2013

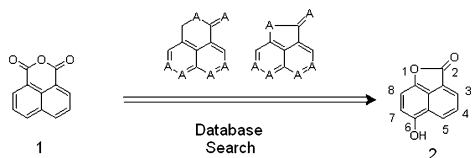
reported studies have generated a number of X-ray crystal structures and binary and ternary complexes of these inhibitors with different TS isoforms (LcTS and *Escherichia coli* TS (EcTS)).<sup>9,10,13</sup> Almost all compounds bind in the MTHF binding site and form binary or ternary complexes with dUMP, suggesting that the inhibitors prevent the binding of both TS substrates, dUMP and MTHF, or MTHF only in the case of ternary complexes. The X-ray crystal structures explain the observed mixed-type inhibition pattern, where the competition with the inhibitor is exploited toward both substrates, resulting in binary complexes. In some cases, the chemical diversity of the new inhibitors explores novel binding sites that are different from the substrate binding sites, as in the case of a156-LcTS (PDB code 1TSL). Almost all the TS inhibitors are lipophilic, with a limited number of hydrogen bonds established with the binding site. Consequently, the compounds float in the large TS active site, accounting for the multiple binding modes. Among all the studied structures, drastic structural changes have never been observed.

Continuing the search for new series of compounds with higher specificity toward pathogenic enzymes with respect to the human TS, we extended our studies to a larger enzyme panel that included 5 TS enzyme isoforms, among them the lesser studied *Pneumocystis carinii* TS (PcTS) and *Enterococcus faecalis* TS (EfTS). We performed a deconstruction approach starting from 1,8-NPTH carboxamide derivatives (Scheme 1). Here, we describe the identification of a new scaffold molecule and the design and syntheses of a small molecular library. These novel compounds were tested for their enzymatic inhibition activity, and the X-ray crystallographic structure of EcTS in complex with one of the compounds is reported. For the first time, a novel TS binding site is shown in which dUMP is displaced from its classical active site in the ternary complex.

## RESULTS

**Scaffold Identification: Database Search, Scaffold Selection.** We aimed to discover new possible scaffolds starting from 1,8-naphthalic anhydride (**1**). Scifinder was searched using the substructure search method (see Supporting Information for details). A number of possible scaffolds emerged, and **2** was chosen for further synthetic elaboration (Scheme 2).

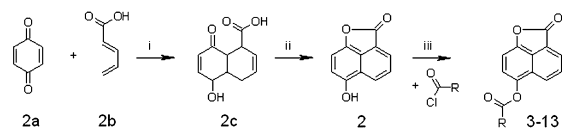
### Scheme 2. Database Queries and Scaffold Identification



**Scaffold Synthesis, Library Design, and In-Parallel Synthesis.** The scaffold synthesis began with the Diels–Alder reaction of commercially available 1,4-benzoquinone (**2a**) and penta-2,4-dienoic acid (**2b**) in toluene at 80 °C (Scheme 3), yielding 5,8-dioxo-1,4,4a,5,8a-hexahydronaphthalene-1-carboxylic acid (**2c**). This compound was converted to 6-hydroxy-2H-naphtho[1,8-*bc*]furan-2-one (**2**) in a one-pot reaction via *p*-toluenesulfonic acid mediated lactonization and Pd/C catalyzed aromatization.<sup>15</sup>

The phenolic oxygen of **2** was selected for in-parallel chemistry approaches.

### Scheme 3. Scaffold (**2**): Synthesis and Derivatization<sup>a</sup>



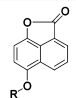
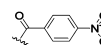
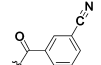
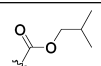
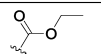
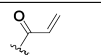
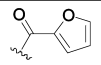
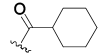
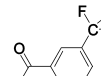
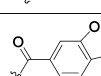
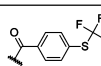
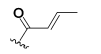
<sup>a</sup>(i) Toluene, 80 °C; (ii) toluene, *p*-toluenesulfonic acid, Pd/C, reflux; (iii) toluene, triethylamine, reflux.

A small library of ester derivatives was then designed and synthesized. A set of acyl chlorides was selected for the esterification of the hydroxyl group at position 6 (see Supporting Information for details). Their molecular weights ranged from 238 to 394 Da; their log *P* values ranged from 2.75 to 5.46, and their solubilities, expressed as log(1/(solubility [mol/L])), ranged from 3.9 to 7.8. Compounds **3–13** were synthesized in refluxing toluene at 110 °C using triethylamine as an acid scavenger<sup>16</sup> (Scheme 3).

**Biological Activity.** Compounds **3–13** were tested against a TS-based enzyme biolibrary including EcTS, PcTS, EfTS, LcTS, and hTS (Table 1).

The  $K_{i\text{EcTS}}$  values ranged between 4 and 67  $\mu\text{M}$ . Only **3** and **4** showed values of <10  $\mu\text{M}$ . The  $K_{i\text{EfTS}}$  values ranged between

**Table 1.** Inhibition Activity Profile ( $K_i$  ( $\mu\text{M}$ )) of Synthesized Compounds<sup>a</sup>

	EcTS	EffTS	LcTS	PcTS	hTS
R					
<b>3</b>	 6 ±0.2	27 ±0.7	1.2 ±0.04	3.5 ±0.24	35 ±0.9
<b>4</b>	 4.0 ±0.01	14 ±0.3	0.39 ±0.005	0.31 ±0.009	7 ±0.2
<b>5</b>	 NI	NI	9 ±0.2	NI	NI
<b>6</b>	 67 ±2	37 ±1	10 ±0.3	34 ±0.8	60 ±1.4
<b>7</b>	 19 ±0.6	41 ±1.3	10 ±0.3	19 ±0.4	8 ±0.7
<b>8</b>	 NI	20 ±0.3	13 ±0.2	15 ±0.2	28 ±0.4
<b>9</b>	 66 ±0.9	NI	49 ±0.7	18 ±0.2	NI
<b>10</b>	 NI	41 ±0.8	33 ±0.5	NI	NI
<b>11</b>	 NI	NI	NI	NI	NI
<b>12</b>	 NI	NI	NI	NI	NI
<b>13</b>	 NI	NI	6 ±0.1	10 ±0.3	NI

<sup>a</sup>The  $K_i$  values are expressed as the mean ± SEM of three determinations.

14 and 41  $\mu\text{M}$ , and **4** was the best inhibitor. The  $K_{\text{i, EcTS}}$  values ranged between 0.39 and 49  $\mu\text{M}$ . Compounds **3**, **4**, **5**, **6**, **7**, and **13** exhibited  $K_{\text{i}}$  values of  $\leq 10 \mu\text{M}$ . The  $K_{\text{i, PcTS}}$  values ranged between 0.31 and 34  $\mu\text{M}$ . Compounds **3**, **4**, and **13** showed values of  $\leq 10 \mu\text{M}$ . The  $K_{\text{i, hTS}}$  values ranged between 7 and 60  $\mu\text{M}$ . Compounds **4** and **7** demonstrated  $K_{\text{i}}$  values of  $\leq 10 \mu\text{M}$ .

The most active molecule was **4**, which exhibited the lowest  $K_{\text{i}}$  against all the tested enzymes, and in particular, it showed a nanomolar  $K_{\text{i, PcTS}}$  with a specificity index ( $\text{SI} = K_{\text{i, hTS}}/K_{\text{i, PcTS}}$ ) of  $>20$ . Other interesting compounds were **9** and **13**, which were active against PcTS ( $K_{\text{i, PcTS}}$  of 18 and 10  $\mu\text{M}$ , respectively) and specific with respect to hTS. These molecules did not inhibit hTS at 100  $\mu\text{M}$ .

**X-ray Crystallographic Studies.** Compounds **3** and **4** exhibited the best activity profiles (their  $K_{\text{i}}$  values against TS from microorganisms are always the lowest or among the lowest values) and were selected for X-ray crystallography studies with PcTS and EcTS. Only a crystallographic structure of a ternary complex of **3** with EcTS and dUMP was obtained (Table S1 and Supporting Information). Previous X-ray crystallographic studies by Anderson et al.<sup>17</sup> revealed that PcTS shows a strong coupling between the two monomers forming the dimer, thus explaining the observed negative cooperativity.<sup>17</sup> PcTS unique structural features could lead to unsuitable crystals in complex with our selected compounds.

**EcTS–dUMP–**3** Ternary Complex.** The EcTS–dUMP–**3** (PDB code 4LRR) complex maintained the same structure as the native enzyme (PDB code 3TMS; PDB code 1F4B), having a root-mean-square deviation of only 0.37 Å between the backbone atoms of the two structures.<sup>18,19</sup>

The  $\Delta F$  map shows electron density that is well above noise and is compatible with the presence of the naphthofuranosyl ring of **3**, located near the Cys146 sulfur (at  $\sim 3.3$  Å) in a hydrophobic environment defined by Trp80, Trp83, Leu143, Ile79, and Tyr94 (Figure 1). The same electron density map does not exhibit any features attributable to a dUMP molecule bound in the active site. However, positive electron density compatible with a ribose ring is clearly visible. This positive electron density is elongated from the usual phosphate binding site of dUMP, located between Arg21–Arg166 of one subunit and Arg126'–Arg127' of the symmetry related subunit in the

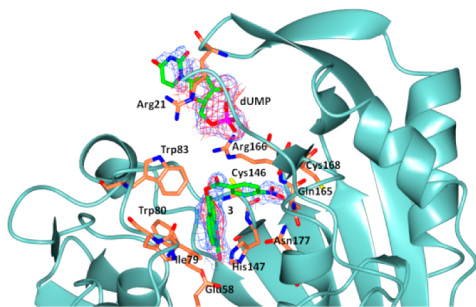


**Figure 1.** View of the EcTS–dUMP–**3** ternary complex (PDB code 4LRR). The electron density around **3** and dUMP is from an omit map computed with phases from the refined model without the inhibitor and substrate and contoured at  $3.0\sigma$  (red) superimposed on the  $2F_o - F_c$  map contoured at  $1.0\sigma$  (blue). **3** and dUMP are represented in CPK colors (green, carbon atoms), while the enzyme is represented as a sea green ribbon. The side chains of the residues involved in contacts with **3** and dUMP are shown as sticks (coral, carbon atoms). The catalytic Cys146 residue is also shown behind **3**. Water molecules have been omitted for clarity.

EcTS dimer and extends with the nucleoside moiety outside the active site cavity toward the solvent and H-bonded to Asp122', as shown in Figure S1 (see Supporting Information).

A similar dUMP binding mode was previously observed by Lebioda and collaborators for the analogue FdUMP, which was cocrystallized with a Val3Phe mutant of hTS (PDB code 3EJL).<sup>20</sup> In this instance, these authors showed that the Val3Phe mutation strongly compromised the dUMP binding capability to hTS. Our results indicate that bulky inhibitors such as **3**, able to occupy a large portion of the active site close to Cys146, also do not allow the binding of dUMP within the active site (Figure S2, Supporting Information).

**Implication for Further Drug Design.** The ternary complex structure of EcTS–dUMP–**3** makes it possible to define the binding site for this family of inhibitors and to identify a novel binding mode for dUMP. This binding mode occludes most of the EcTS cavity, preventing access to the catalytic Cys146 and simultaneously hindering the binding of dUMP within the active site. Contrastingly, the benzoyl moiety of these molecules appears to be devoid of chemical determinants that can form specific interactions within the EcTS cavity. In the structure, this region of the inhibitor is poorly defined, and multiple binding modes appear to be possible.

The crystal structure of the complex described highlights how the naphthofuranosyl moiety can be used as a scaffold to design more potent TS inhibitors and suggests the use of the polar groups present in the active site cavity, such as Glu58, Tyr94, His147 and Asn177, to achieve a higher binding affinity. The observed binding of dUMP also suggests that “surface” inhibitors of EcTS might be designed by starting from the phosphate binding site and exploiting the contacts shown by dUMP at the surface of the EcTS dimer, with residues such as Asp122', Asp124', and Ser125'.

## CONCLUSION

In searching for novel specific inhibitors of bacterial TS enzymes, we combined a ligand-based design with X-ray crystallographic studies to characterize the binding modes of the active compounds.

Through the derivatization of scaffold **2**, we obtained nine active compounds. The most active molecule was **4**, which exhibited the lowest  $K_{\text{i}}$  values against all of the tested enzymes and in particular exhibited a nanomolar level  $K_{\text{i, PcTS}}$  with a specificity index ( $\text{SI} = K_{\text{i, hTS}}/K_{\text{i, PcTS}}$ ) of  $>20$ . Other interesting and specific compounds were **9** and **13**, which inhibited PcTS ( $K_{\text{i, PcTS}}$  of 18 and 10  $\mu\text{M}$ , respectively) but showed no inhibition of hTS at 100  $\mu\text{M}$ . These compounds can be exploited to improve the inhibition profile. The most remarkable structural aspect was that of **3**, which could be crystallized with EcTS in a ternary complex. A novel binding mode was observed in this complex, with dUMP displaced from its binding site. The  $\Delta F$  map indicated that this inhibitor is able to occupy a large portion of the active site close to Cys146, preventing the binding of dUMP within it. Thus, dUMP appears to be bound at the interface between the two symmetry-related subunits of the dimeric enzyme structure, revealing a new binding site for the substrate. The kinetic experiments supported the concept of a mixed-type inhibition pattern with respect to the substrates. The binding mode observed for this compound series is a key feature that has not been observed with any other TS inhibitor previously explored and could introduce new opportunities for the design of novel



species-specific compounds directed against pathogenic TS. The concept here presented can be of general interest for understanding the structural basis of specificity of lead compounds.

## EXPERIMENTAL SECTION

**Chemistry.** The reagents were purchased from Sigma-Aldrich and used without further purification. The reaction progress was monitored using TLC on precoated silica gel 60 F254 plates (Merck) and visualized with UV light (254 nm). The purity of all materials was determined to be at least 95% via TLC,  $^1\text{H}$  NMR, and elemental analyses. The synthesis of 3–13 was performed using a Büchi Syncore parallel synthesizer with yields in the range of 30–45%. The elemental analyses were performed on a Perkin-Elmer 240C instrument, and the results for C, H, and N were within  $\pm 0.4\%$  of the theoretical values. All of the synthesized compounds were characterized with  $^1\text{H}$  NMR on a Bruker DPX-200 MHz spectrometer operating at 200 MHz in  $\text{DMSO}-d_6$ . The chemical shifts are reported as  $\delta$  values (ppm), and the  $J$  values are given in Hz. When peak multiplicities are reported, the following abbreviations are used: s, singlet; d, doublet; t, triplet; q, quartet; m, multiplet; dd, double doublet; br, broad peak.

**5,8-Diketo-1,4,4a,5,8,8a-hexahydronaphthalene-1-carboxylic Acid (2c).** Reagents 1,4-benzoquinone (2a) (2.0 g, 18 mmol) and 2,4-pentadienoic acid (2b) (1.8 g, 18 mmol) were suspended in toluene (80 mL) and heated at  $80^\circ\text{C}$  for 24 h. The mixture was hot-filtered, and the obtained solid was washed with toluene and dried under vacuum. Yield: 0.88 g, 24%.  $^1\text{H}$  NMR  $\delta$  6.85 (1H, d,  $J$  9.0), 6.75 (1H, d,  $J$  9.0), 6.30 (1H, m), 5.80 (1H, m), 4.25 (1H, t,  $J$  6.0), 3.40 (2H, m), 2.35 (1H, m), 2.25 (1H, m). Anal. Calcd for  $\text{C}_{11}\text{H}_{12}\text{O}_4$ : C, 63.45; H, 5.81. Found: C, 63.27; H, 5.84.

**6-Hydroxy-2H-naphtho[1,8-bc]furan-2-one (2).** Compound 2c (0.57 g, 2.8 mmol) was suspended in toluene (57 mL) and stirred for 1 h at  $120^\circ\text{C}$ . *p*-Toluenesulfonic acid (0.64 g, 3.4 mmol) was added, and the mixture was heated at  $120^\circ\text{C}$  for 4 h. After this time, 5% Pd/C (0.035 g) was added and left stirring for 12 h at the same temperature. The reaction mixture was cooled to  $40\text{--}50^\circ\text{C}$  and filtered over a Celite pad, washing the solid with hot toluene. The filtered mixture was concentrated under reduced pressure, and the obtained residue was suspended in 0.5 M  $\text{NaHCO}_3$  and extracted with diethyl ether. The collected organic phases were dried over  $\text{Na}_2\text{SO}_4$  and concentrated under reduced pressure. Yield: 0.39 g, 75.4%.  $^1\text{H}$  NMR  $\delta$  10.55 (1H, s), 8.50 (1H, d,  $J$  8.0), 8.35 (1H, d,  $J$  8.1), 8.00 (1H, t,  $J$  8.0), 7.30 (1H, d,  $J$  8.0), 7.00 (1H, d,  $J$  7.9). Anal. Calcd for  $\text{C}_{11}\text{H}_6\text{O}_3$ : C, 70.97; H, 3.25. Found: C, 70.82; H, 3.19.

**General Method for Preparing 3–13.** Compound 2 (0.04 g, 0.2 mmol) was suspended in toluene (8 mL). The appropriate acyl chloride (0.4 mmol) and triethylamine (0.5 mL, 3.6 mmol) were then sequentially added to the solution, and the mixture was stirred at 280 rpm for 24 h and heated at  $110^\circ\text{C}$  in a Büchi Syncore parallel synthesizer.<sup>16</sup> After reaction completion, the mixture was filtered, and the filtrate was worked up with a 0.5 M  $\text{NaHCO}_3$  solution. The organic phase was then dried over  $\text{Na}_2\text{SO}_4$ , the solvent evaporated under reduced pressure, and the obtained residue purified using column chromatography ( $\text{CH}_2\text{Cl}_2/\text{CH}_3\text{OH}$  9:1).

**6-(4-Nitrobenzoyloxy)-2-oxo-2H-naphtho[1,8-bc]furan (3).**  $^1\text{H}$  NMR  $\delta$  8.58 (4H, m), 8.49 (1H, d,  $J$  1.2), 8.45 (1H, d,  $J$  2.4), 8.05–8.15 (1H, dd,  $J$  8.4,  $J$  6.4), 7.78 (1H, d,  $J$  8.4), 7.56 (1H, d,  $J$  8.4). Anal. Calcd for  $\text{C}_{18}\text{H}_9\text{NO}_6$ : C, 64.48; H, 2.71; N, 4.18. Found: C, 64.26; H, 2.64; N, 4.16.

**6-(3-Cyanobenzoyloxy)-2-oxo-2H-naphtho[1,8-bc]furan (4).**  $^1\text{H}$  NMR  $\delta$  8.79 (1H, br s), 8.64 (1H, d,  $J$  7.0), 8.47 (1H, d,  $J$  2.0), 8.45 (1H, d,  $J$  1.0), 8.37 (1H, d,  $J$  7.0), 8.08 (1H, d,  $J$  7.0), 7.98 (1H, d,  $J$  7.0), 7.75 (1H, d,  $J$  7.0), 7.55 (1H, d,  $J$  7.0). Anal. Calcd for  $\text{C}_{19}\text{H}_9\text{NO}_4$ : C, 72.38; H, 2.88; N, 4.44. Found: C, 72.29; H, 2.83; N, 4.39.

**TS Activity Inhibition Profile Evaluation.** See Supporting Information.

**Crystallization Conditions.** See Supporting Information.

**Data Collection, Processing, and Structure Determination.** See Supporting Information.

## ASSOCIATED CONTENT

### Supporting Information

Details of scaffold identification, library design, X-ray structure analyses, data collection and refinement statistics, experimental methods, NMR, and C, H, and N microanalyses for the synthesized compounds. This material is available free of charge via the Internet at <http://pubs.acs.org>.

### Accession Codes

PDB code for EcTS–dUMP–3 complex: 4LRR.

## AUTHOR INFORMATION

### Corresponding Author

\*Phone: 0039-059-205-5134. Fax: 0039-059-205-5131. E-mail: [mariapaola.costi@unimore.it](mailto:mariapaola.costi@unimore.it).

### Present Address

<sup>§</sup>R.L.: Hammerstrasse 50, 4058 Basel Switzerland.

### Author Contributions

All authors have given approval to the final version of the manuscript.

### Notes

The authors declare no competing financial interest.

## ACKNOWLEDGMENTS

The authors acknowledge the grant of the project PRIN 2009 to M.P.C. The authors thank Prof. Rinaldi Marcella for her support of the synthetic study.

## ABBREVIATIONS USED

ADP, atomic displacement parameter; DMSO, dimethylsulfoxide; dTMP, 2'-deoxythymidine 5'-monophosphate; dUMP, 2'-deoxyuridine 5'-monophosphate; EcTS, *Escherichia coli* thymidylate synthase; EftTS, *Enterococcus faecalis* thymidylate synthase; FdUMP, 5-fluorodeoxyuridine 5'-monophosphate; hTS, human thymidylate synthase;  $K_i$ , inhibition constant; LcTS, *Lactobacillus casei* thymidylate synthase; MTHF, N<sup>5</sup>,N<sup>10</sup>-methylene tetrahydrofolate; PTH, phenolphthalein; PcTS, *Pneumocystis carinii* thymidylate synthase; SI, specificity index; TS, thymidylate synthase

## REFERENCES

- (1) Costi, M. P.; Ferrari, S.; Venturelli, A.; Calò, S.; Tondi, D.; Barlocco, D. Thymidylate synthase structure, function and implication in drug discovery. *Curr. Med. Chem.* **2005**, *12*, 2241–2258.
- (2) Jarmula, A. Antifolate inhibitors of thymidylate synthase as anticancer drugs. *Mini-Rev. Med. Chem.* **2010**, *10*, 1211–1222.
- (3) Garg, D.; Henrich, S.; Salo-Ahen, O. M.; Myllykallio, H.; Costi, M. P.; Wade, R. C. Novel approaches for targeting thymidylate synthase to overcome the resistance and toxicity of anticancer drugs. *J. Med. Chem.* **2010**, *53*, 6539–6549.
- (4) Shoichet, B. K.; Stroud, R. M.; Santi, D. V.; Kuntz, I. D.; Perry, K. M. Structure-based discovery of inhibitors of thymidylate synthase. *Science* **1993**, *259*, 1445–1450.
- (5) Ghelli, S.; Rastelli, G.; Barlocco, D.; Rinaldi, M.; Tondi, D.; Pecorari, P.; Costi, M. P. Conformational analysis of phthalein derivatives acting as thymidylate synthase inhibitors by means of  $^1\text{H}$  NMR and quantum chemical calculations. *Bioorg. Med. Chem.* **1996**, *4*, 1783–1794.
- (6) Ferrari, S.; Costi, M. P.; Wade, R. Inhibitor specificity via protein dynamics: insights from the design of antibacterial agents targeted against thymidylate synthase. *Chem. Biol.* **2003**, *10*, 1183–1193.

- (7) Costi, M. P.; Gelain, A.; Barlocco, D.; Ghelli, S.; Soragni, F.; Reniero, F.; Rossi, T.; Ruberto, A.; Guillou, C.; Cavazzuti, A.; Casolari, C.; Ferrari, S. Antibacterial agent discovery using thymidylate synthase biolibrary screening. *J. Med. Chem.* **2006**, *49*, 5958–5968.
- (8) Costi, M. P.; Tondi, D.; Rinaldi, M.; Barlocco, D.; Pecorari, P.; Soragni, F.; Venturelli, A.; Stroud, R. M. Structure-based studies on species-specific inhibition of thymidylate synthase. *Biochim. Biophys. Acta* **2002**, *1587*, 206–214.
- (9) Stout, T. J.; Tondi, D.; Rinaldi, M.; Barlocco, D.; Pecorari, P.; Santi, D. V.; Kuntz, I. D.; Stroud, R. M.; Shoichet, B. K.; Costi, M. P. Structure-based design of inhibitors specific for bacterial thymidylate synthase. *Biochemistry* **1999**, *38*, 1607–1617.
- (10) Finer-Moore, J. S.; Anderson, A. C.; O'Neil, R. H.; Costi, M. P.; Ferrari, S.; Krucinski, J.; Stroud, R. M. The structure of *Cryptococcus neoformans* thymidylate synthase suggests strategies for using target dynamics for species-specific inhibition. *Acta Crystallogr., Sect. D: Biol. Crystallogr.* **2005**, *D61*, 1320–1334.
- (11) Benassi, L.; Magnoni, C.; Giudice, S.; Bertazzoni, G.; Costi, M. P.; Rinaldi, M.; Venturelli, A.; Coppi, A.; Rossi, T. Pharmacological and toxicological evaluation of a new series of thymidylate synthase inhibitors as anticancer agents. *Anticancer Res.* **2006**, *26*, 3499–3504.
- (12) Giudice, S.; Benassi, L.; Bertazzoni, G.; Veratti, E.; Morini, D.; Azzoni, P.; Costi, M. P.; Venturelli, A.; Pirondi, S.; Seidenari, S.; Magnoni, C. Biological evaluation of MR36, a novel non-polyglutamatable thymidylate synthase inhibitor that blocks cell cycle progression in melanoma cell lines. *Invest. New Drugs* **2012**, *30*, 1484–1492.
- (13) Mangani, S.; Cancian, L.; Leone, R.; Pozzi, C.; Lazzari, S.; Luciani, R.; Ferrari, S.; Costi, M. P. Identification of the binding modes of *N*-phenylphthalimides inhibiting bacterial thymidylate synthase through X-ray crystallography screening. *J. Med. Chem.* **2011**, *54*, 5454–5467.
- (14) Ferrari, S.; Ingrams, M.; Soragni, F.; Wade, R. C.; Costi, M. P. Ligand-based discovery of *N*-(1,3-dioxo-1*H*,3*H*-benzo[*de*]isochromen-5-yl)-carboxamide and sulfonamide derivatives as thymidylate synthase A inhibitors. *Bioorg. Med. Chem. Lett.* **2013**, *23*, 663–668.
- (15) Sabie, R.; Fillion, H.; Daudon, M.; Pinatel, H. A regiospecific synthesis of  $\alpha$ -acetyl- $\alpha'$ -naphthols via a Diels–Alder reaction. *Synth. Commun.* **1990**, *20*, 1713–1719.
- (16) Bouaziz, Z.; Fillion, H. Synthesis of 5-carbamoyloxy- and 5-acyloxynaphthalene-1,8-carbolactones with potential antitumoral activity. *Pharmazie* **1989**, *44*, 226–227.
- (17) Anderson, A. C.; O'Neil, R. H.; DeLano, W. L.; Stroud, R. M. The structural mechanism for half-the-sites reactivity in an enzyme, thymidylate synthase, involves a relay of changes between subunits. *Biochemistry* **1999**, *38*, 13829–13836.
- (18) Perry, K. M.; Fauman, E. B.; Finer-Moore, J. S.; Montfort, W. R.; Maley, G. F.; Maley, F.; Stroud, R. M. Plastic adaptation toward mutations in proteins: structural comparison of thymidylate synthases. *Proteins* **1990**, *8*, 315–333.
- (19) Erlanson, D. A.; Braisted, A. C.; Raphael, D. R.; Randal, M.; Stroud, R. M.; Gordon, E. M.; Wells, J. A. Site-directed ligand discovery. *Proc. Natl. Acad. Sci. U.S.A.* **2000**, *97*, 9367–9372.
- (20) Huang, X.; Gibson, L. M.; Bell, B. J.; Lovelace, L. L.; Peña, M. M.; Berger, F. G.; Berger, S. H.; Lebioda, L. Replacement of Val3 in human thymidylate synthase affects its kinetic properties and intracellular stability. *Biochemistry* **2010**, *49*, 2475–2482.